



THE UNIVERSITY *of* EDINBURGH

Edinburgh Research Explorer

Saturated Pressure Measurements of 2,3,3,3-Tetrafluoroprop-1-ene (HFO-1234yf)

Citation for published version:

Di Nicola, G, Polonara, F & Santori, G 2010, 'Saturated Pressure Measurements of 2,3,3,3-Tetrafluoroprop-1-ene (HFO-1234yf)', *Journal of Chemical and Engineering Data*, vol. 55, no. 1, pp. 201-204.
<https://doi.org/10.1021/je900306v>

Digital Object Identifier (DOI):

[10.1021/je900306v](https://doi.org/10.1021/je900306v)

Link:

[Link to publication record in Edinburgh Research Explorer](#)

Document Version:

Peer reviewed version

Published In:

Journal of Chemical and Engineering Data

Publisher Rights Statement:

This document is the unedited author's version of a Submitted Work that was subsequently accepted for publication in *Journal of Chemical and Engineering Data*, copyright © American Chemical Society after peer review. To access the final edited and published work, see <http://pubs.acs.org/doi/abs/10.1021/je900306v>.

General rights

Copyright for the publications made accessible via the Edinburgh Research Explorer is retained by the author(s) and / or other copyright owners and it is a condition of accessing these publications that users recognise and abide by the legal requirements associated with these rights.

Take down policy

The University of Edinburgh has made every reasonable effort to ensure that Edinburgh Research Explorer content complies with UK legislation. If you believe that the public display of this file breaches copyright please contact openaccess@ed.ac.uk providing details, and we will remove access to the work immediately and investigate your claim.



Saturated Pressure Measurements of 2,3,3,3-Tetrafluoroprop-1-ene (HFO-1234yf)

Giovanni Di Nicola, Fabio Polonara, Giulio Santori

Dipartimento di Energetica, Università Politecnica delle Marche,

Via Brecce Bianche, 60100 Ancona, Italy

Abstract

The vapor pressure data of 2,3,3,3-Tetrafluoroprop-1-ene ($\text{CF}_3\text{CF}=\text{CH}_2$, HFO-1234yf) were measured using a constant volume apparatus. Measurements were carried out in a wide temperature range, from (224 to 366) K, and at pressures from (39 to 3218) kPa. A total of 35 experimental points were obtained. The measurements were fitted to the Wagner equation with an absolute deviation of 0.35 %. To our knowledge, no other experimental results have been published in the open literature on the properties studied here; for this reason our experimental results were compared with a preliminary equation of state.

tel:+39-0712204277

fax:+39-0712204770

Email: g.dinicola@univpm.it

Introduction

In order to solve the depletion of the ozone layer problem, ChloroFluoroCarbons (CFCs) have been phased out and HydroChloroFluoroCarbons (HCFCs) will be phased out according to the Montreal Protocol time frame. HydroFluoroCarbons (HFCs) has been chosen as new refrigerants with no ozone depletion, but they have been included in the classified greenhouse gases list by the Kyoto Protocol as contributors to the climate change. For a lower impact on the environment, the European Union decided to ban refrigerants with Global Warming Potential (GWP) over 150 in automobile air conditioning. This sector thus needs to find alternatives to the currently used fluid, R-134a (GWP=1430 for a 100 years time horizon). During the last decade several refrigerants have been evaluated as possible options in automobile air conditioning either natural refrigerants (i.e., R-744, carbon dioxide) and synthetic refrigerants.^{1,2}

Although R-744 has a GWP=1 and an Ozone Depletion Potential (ODP) that is zero, it has some restrictions due to its thermophysical properties. Additionally, technical issues regarding the use of carbon dioxide in mobile air conditioning remain unresolved by the industry and the very high system pressures require total redesign of just about every system component. For these reasons, R-744 has been challenged as the ideal refrigerant for automobile air condition application.

DuPont and Honeywell recently proposed a new refrigerant to replace R-134a, a HydroFluoroOlefin called HFO-1234yf ($\text{CF}_3\text{CF}=\text{CH}_2$, 2,3,3,3-Tetrafluoroprop-1-ene) that offers thermophysical proprieties similar to R-134a and for this reason requires minimum equipment changes. The same refrigerant has been presented by another chemical manufacturer, the French group Arkema in a Congress which was held in Austria last February.³

This fluid is mildly flammable, having a small gap between lower and upper flammability limits. It is also thermally stable with no significant corrosion to metals. It is a non-ozone-depleting substance, having an atmospheric lifetime of 11 days. It also has the lowest Life-Cycle Climate

Performance (LCCP) compared to both R-134a and R-744.⁴ Its GWP is approximately 12 for a 20 years time horizon and 4 for a 100 years time horizon.⁵

Regarding toxicity, the data demonstrate a low potential, similar to R-134a, by tests on male rats and mice.⁶ Considering the ATEL (Acute Toxicity Exposure Limit), HFO-1234yf also has a favourable ATEL value (101000 ppm).

HFO-1234yf thermodynamic properties are very similar to R-134a: boiling point, critical point, and liquid and vapour density are comparable to R-134a.⁷

In spite of all these considerations, to our best knowledge very few experimental data on the thermophysical properties of this fluid have been published so far in the open literature.

In this paper, the vapour pressure region properties of this fluid were measured in the two phase region by means on an isochoric apparatus. Data were collected over a wide temperature range, from (224 to 366) K. Experimental results were regressed with the Wagner equation and compared with REFPROP 8.0 prediction,⁸ with a preliminary equation developed with these data.⁹

Experimental Section

Materials. The sample was produced by the French group Arkema and donated by Centro Ricerche FIAT, Italy. It was then degassed to remove air and other non condensable gases by immersing it in liquid nitrogen and evacuating. It was then brought to room temperature and was again subjected to freezing, evacuating and thawing process. This procedure was repeated several times. Its purity was checked by gas chromatography using a thermal conductivity detector and was found to be better than 99.95 % on a molar basis by analysis of peak area.

Apparatus. The new experimental setup is illustrated in Figure 1. The basic experimental setup has already been described elsewhere,¹⁰ so it is only briefly outlined here. Two twin thermostatic baths were filled with different silicone oils (Baysilone M10 and Baysilone M100, Bayer). After charging with the sample, the setup could be operated over two temperature ranges, approximately from (210 to 290) K and from (290 to 360) K, depending on which bath was used. The two silicone oils have

different kinematic viscosity values (10 and 100 cSt at room temperature, respectively). The one with lower kinematic viscosity, due to its higher volatility, was applied only for the low temperature range, while that with a greater viscosity was applied only at high temperatures. The thermostatic baths were easy to move thanks to the new system configuration. The spherical cells and pressure transducer are immersed in one of the two thermostatic baths. An auxiliary thermostat was used to reach below-ambient temperatures. The cell volume was estimated to be $(273.5 \pm 0.3) \text{ cm}^3$ at room temperature¹⁰ and the cell volume change with temperature was taken into account.^{11,12} The pressure and temperature data acquisition systems were identical to those of the previous apparatus.^{11,12} A PID device was used to control the temperature, which was measured using a resistance thermometer. The temperature of the sample was measured by a platinum resistance (mod. Hart 25 Ω), calibrated in accordance with ITS 90 at Istituto di Metrologia “G. Colonnetti” in Turin (Italy). The total uncertainty of the temperature measurements was $\pm 0.02 \text{ K}$. The pressure in the sample was transduced to the manometer through the diaphragm type differential pressure transducer (mod. Ruska 2413) coupled with an electronic null indicator (mod. Ruska 2416). The uncertainty in the pressure measurements stems from the uncertainty of the transducer and null indicator system, and the pressure gauges. The uncertainty of the digital pressure indicator (Ruska, mod. 7000) is $\pm 0.003 \%$ of its full scale. Temperature fluctuations due to bath instability can also affect the total uncertainty in the pressure measurement, which was nonetheless found to be less than $\pm 1 \text{ kPa}$. The charging procedure by gravimetric method has also been described elsewhere.¹³

Results and Discussion

Excluding a few points,^{7,14} no published data were available in the open literature for HFO-1234yf. For this reason, seven vapor pressure points were taken for R-134a in the same temperature range (from 243 K to 353 K) of the measurements taken for HFO-1234yf to check the reliability of the experimental setup. This fluid was chosen as a reference because of its very well known thermophysical properties, and the Tillner-Roth equation of state¹⁵ implemented in REFPROP 8.0 is

able to calculate vapor pressure data for R-134a with typical uncertainties of 0.02 %. In Table 1 the experimental vapor pressure data for R-134a are reported together with data calculated by REFPROP 8.0 calculations. The measured data were within the uncertainty values of the equation of state.

At the saturation state, 35 points were obtained in the two phase region for HFO-1234yf. The present experimental vapor pressures measured at temperatures in the range (224 to 366) K are given in Table 2.

Experimental data were fit to the four-parameter Wagner equation:

$$\ln \frac{P}{P_c} = \frac{T_c}{T} [A_1 \tau + A_2 \tau^{1.5} + A_3 \tau^3 + A_4 \tau^6] \quad (1)$$

where $\tau = (T_c - T)/T_c$; the critical temperature $T_c = 368.15$ K.⁶

The following values were found for the parameters: $A_1 = -7.82239$, $A_2 = -2.15165$, $A_3 = -21.16155$, $A_4 = -26.25422$. During the fitting procedure, the critical pressure was fitted as a parameter and the datum (shown with a “*” in table 2) close to the critical point ($T = 365.93$ K and $P = 3218.4$ kPa) was not considered because it produced much higher deviations,.

Best results were obtained with $P_c = 3389.5$ kPa, a value close to $P_c = 3404$ kPa reported by the preliminary equation of state,^{8,9} and quite far from $P_c = 3240$ kPa.⁷

Defining the deviations in pressure as

$$dP = \frac{1}{n} \sum_{i=1}^n [(P_{\text{exp}} - P_{\text{calc}}) / P_{\text{exp}}] \times 100 \quad (2)$$

$$|dP| = \frac{1}{n} \sum_{i=1}^n |(P_{\text{exp}} - P_{\text{calc}}) / P_{\text{exp}}| \times 100 \quad (3)$$

where n is the number of experimental points, the following values were found: $dP = 0.004 \%$ and $\text{abs}(dP) = 0.11 \%$. The error distribution is shown in Figures 2 and 3. The absolute deviations were found to be well distributed, excluding one point, within ± 1 kPa, while the relative deviations were found to be usually within $\pm 0.25 \%$ and always within $\pm 0.5 \%$.

Our experimental data were also compared with the preliminary equation of state^{8,9} and reported in Figures 4 and 5. Again producing much higher deviations, the datum close to the critical point ($T=365.93$ K and $P=3218.4$ kPa) was not considered in the equation of state fitting procedure. In terms of absolute deviations almost all the experimental data were found to be within ± 1 kPa; in terms of relative deviations data are consistently within $\pm 0.1\%$ with just 5 points well within $\pm 0.5\%$. In figure 6, relative deviations of present measurements from the preliminary equation of state^{8,9} and the few points found in the literature^{7,14} were compared, obtaining deviations between 1 % and 2 %.

Conclusions

The measurements of 35 experimental points for saturated pressure were obtained using a constant-volume apparatus for HFO-1234yf. To check the reliability of the experimental setup, a few experimental vapor pressure points were taken for R-134a in the same temperature range of the present paper measurements, and good consistency with REFPROP 8.0 was found. The experimental points taken in the two phase region were fitted with a Wagner type equation. The experimental data were also compared with a preliminary equation of state developed with these data.

The measured data confirmed that HFO-1234yf is very similar to R134a in terms of vapor pressure: a discrepancy of about 15 kPa at low temperatures (at about 243 K) and of -20 kPa at high temperatures (at about 352 K) was evident. This confirms that the fluid under investigation could be a valuable option in automobile air conditioning.

Acknowledgement

The authors are grateful to Eric W. Lemmon for his kind help.

Figure captions

Figure 1. Schematic illustration of the apparatus.

- | | |
|-------------------------------------|------------------------------------------------|
| 1. Constant volume spherical cell | 12. Power system |
| 2. Auxiliary cell | 13. Cooling coil |
| 3. Magnetic pump | 14. Connections to auxiliary thermostatic bath |
| 4. Differential pressure transducer | 15. Acquisition system |
| 5. Electronic null indicator | 16. Bourdon gage |
| 6. Charging system | 17. Dead weight gage |
| 7. Thermostatic baths | 18. Vibrating cylinder pressure gage |
| 8. Platinum thermo-resistances | 19. Precision pressure controller |
| 9. Thermometric bridge | 20. Nitrogen reservoir |
| 10. Stirrer | 21. Vacuum pump system |
| 11. Heater | |

Figure 2. Scatter diagram of the saturated pressure-absolute deviations between experimental pressures (P_{exp}) and pressures calculated from the fit with the Wagner equation, eq 1 (P_{lcd}).

Figure 3. Scatter diagram of the saturated pressure-relative deviations between experimental pressures (P_{exp}) and pressures calculated from the fit with the Wagner equation, eq 1 (P_{lcd}).

Figure 4. Scatter diagram of the saturated pressure-absolute deviations between experimental pressures (P_{exp}) and pressures calculated from REFPROP 8.0 (P_{lcd}).

Figure 5. Scatter diagram of the saturated pressure-relative deviations between experimental pressures (P_{exp}) and pressures calculated from REFPROP 8.0 (P_{lcd}).

Figure 6. Scatter diagram of the saturated pressure-relative deviations between experimental pressures (P_{exp}) and pressures calculated from REFPROP 8.0 (P_{lcd}); ●, ref 7; ■, ref 14.

References

- [1] Coulomb, D. New refrigerants. Editorial. *Int. J. Refrigeration* **2008**, *31*, 1121-1122.
- [2] Calm, J. M. The next generation of refrigerants – historical review, considerations, and outlook. *Int. J. Refrigeration* **2008**, *31*, 1123-1133.
- [3] <http://www.r744.com/articles/2009-02-16-update-from-saalfelden-1234yf-vs-r744.php>.
- [4] <http://www.epa.gov/cppd/mac/2008-mac-presentation-1209.htm>.
- [5] Nielsen, O. J.; Javadi, M. S.; Sulbaek Andersen, M. P.; Hurley, M. D.; Wallington, T. J.; Singh, R. Atmospheric chemistry of $\text{CF}_3\text{CF}=\text{CH}_2$: kinetics and mechanisms of gas-phase reactions with Cl atoms, OH radicals, and O_3 . *Chem. Phys. Lett.* **2007**, *439*, 18-22.
- [6] Schuster, P.; Bertermann, R.; Snow, T. A.; Han, X.; Rusch, G. M.; Jepson, G. W.; Dekant, W. Biotransformation of 2,3,3,3-tetrafluoroprop-1-ene (HFO-1234yf). *Toxicol. Appl. Pharmacol.* **2008**, *233*, 323–332.
- [7] Minor, B.; Spatz, M. HFO-1234yf low GWP refrigerant update. International Refrigeration and air conditioning conference at Purdue, July 14-17, **2008**, paper 2349, 1-8.
- [8] Lemmon, E. W.; Huber, M. L.; McLinden, M. O. NIST Standard Reference Database 23, Reference Fluid Thermodynamic and Transport Properties (REFPROP), version 8.0 (National Institute of Standards and Technology), **2007**.
- [9] Lemmon, E. W. (National Institute of Standards and Technology), **2007**. Private communication.
- [10] Di Nicola, G.; Polonara, F.; Ricci, R.; Stryjek, R. PVT_x Measurements for the $\text{R116} + \text{CO}_2$ and $\text{R41} + \text{CO}_2$ Systems. New Isochoric Apparatus. *J. Chem. Eng. Data* **2005**, *50*, 312-318.
- [11] Giuliani, G.; Kumar, S.; Zazzini, P.; Polonara, F. Vapor Pressure and Gas Phase PVT Data and Correlation for 1,1,1,-Trifluoroethane (R143a). *J. Chem. Eng. Data* **1995**, *40*, 903-908.

- [12] Giuliani, G.; Kumar, S.; Polonara, F. A Constant Volume Apparatus for Vapour Pressure and Gas Phase P - v - T Measurements: Validation with Data for R22 and R134a. *Fluid Phase Equilib.* **1995**, *109*, 265-279.
- [13] Di Nicola, G.; Giuliani, G.; Polonara, F.; Stryjek, R. Saturated pressure and P - V - T measurements for 1,1,1,3,3,3-hexafluoropropane (R-236fa). *J. Chem. Eng. Data* **1999**, *44*, 696-700.
- [14] <http://www51.honeywell.com/sm/genetron/common/documents/1234yf-MSDS.pdf>.
- [15] Tillner-Roth, R.; Baehr, H.D. An international standard formulation of the thermodynamic properties of 1,1,1,2-tetrafluoroethane (HFC-134a) for temperatures from 170 K to 455 K at pressures up to 70 MPa. *J. Phys. Chem. Ref. Data* **1994**, *23*, 657-729.

Table 1. Experimental Saturation Pressures P at Temperature T_{90} (according to the ITS-90 equipment calibration standard) for R-134a compared with P_{REF} obtained by REFPROP 8.0 prediction.⁷

T_{90}/K	P/kPa	P_{REF}/kPa	$P-P_{REF}/\text{kPa}$
243.10	84.2	84.2	0.0
248.08	106.1	106.0	0.1
263.01	199.4	199.5	-0.1
283.03	413.0	412.9	0.1
303.12	769.5	769.5	0.0
328.05	1488.0	1488.0	0.0
352.93	2620.8	2620.9	-0.1
Avg.			0.0

Table 2. Experimental Saturation Pressures P at Temperature T_{90} (according to the ITS-90 equipment calibration standard) for HFO-1234yf

T_{90}/K	P/kPa	T_{90}/K	P/kPa
224.12	38.9	297.97	679.4
228.21	48.3	303.12	783.2
233.12	62.0	308.11	894.6
234.21	65.5	313.09	1018.0
238.08	78.7	315.59	1083.5
243.03	98.8	318.08	1153.0
247.95	121.7	320.61	1224.0
252.91	149.2	323.11	1301.1
255.49	165.3	325.58	1380.0
257.70	180.4	333.06	1638.3
258.61	186.9	338.05	1831.0
263.14	221.7	343.02	2039.0
268.10	265.1	348.01	2265.6
272.98	313.9	352.98	2511.5
277.96	370.5	357.97	2778.2
283.09	437.1	362.94	3067.1
288.08	509.4	365.93*	3218.4*
292.87	587.3		

*not considered in the regression.

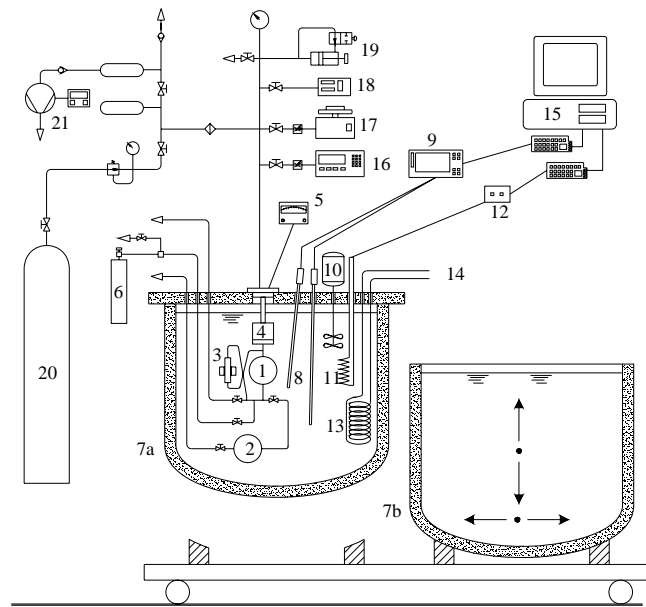


Figure 1

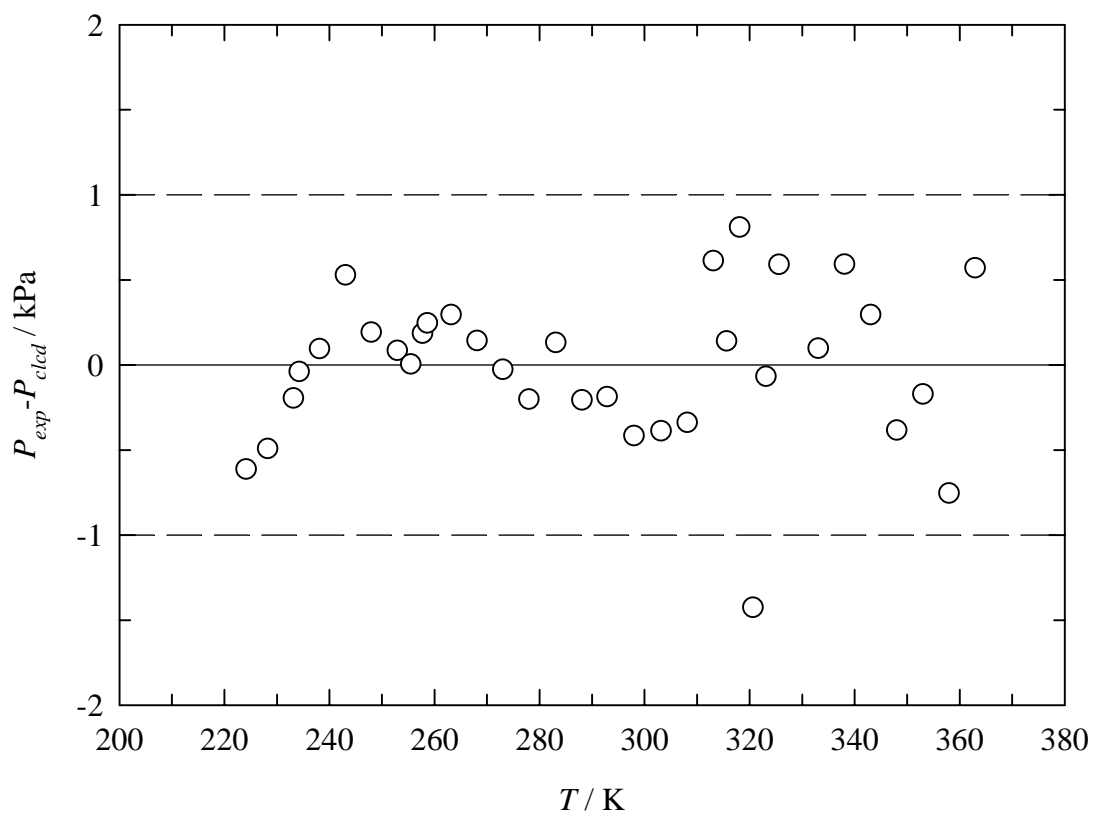


Figure 2.

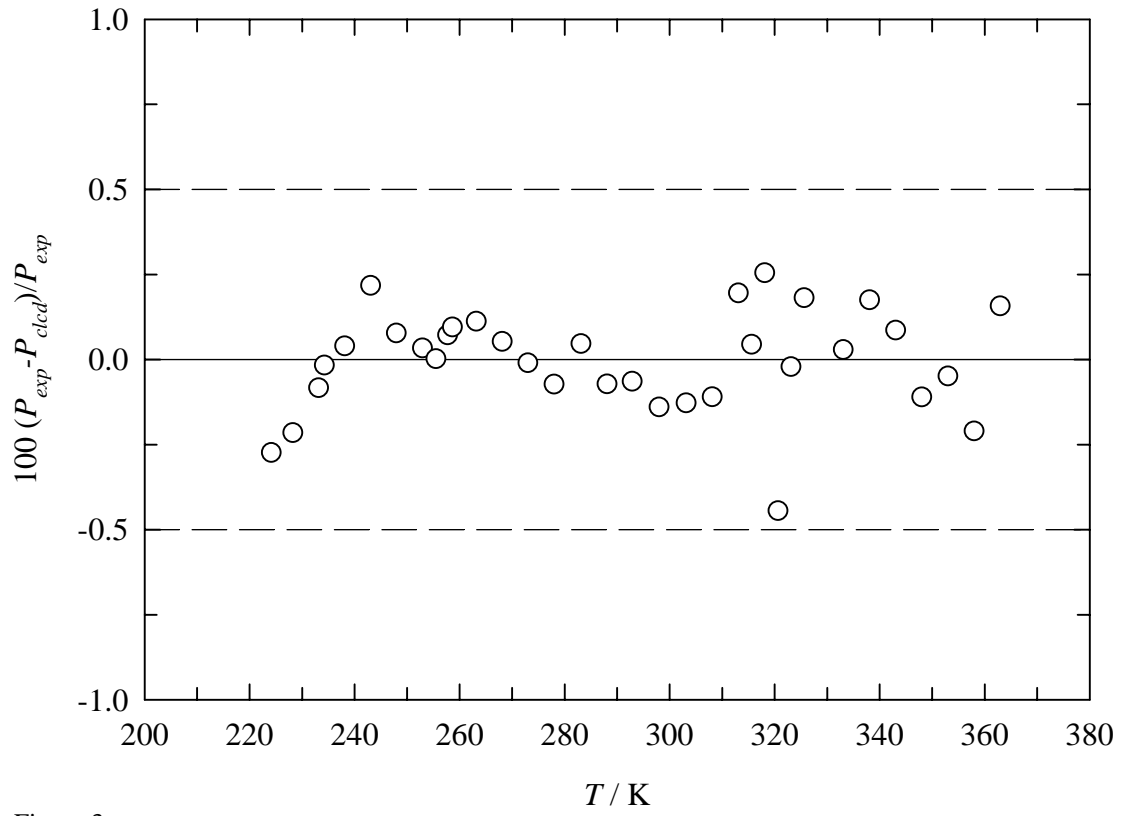


Figure 3.

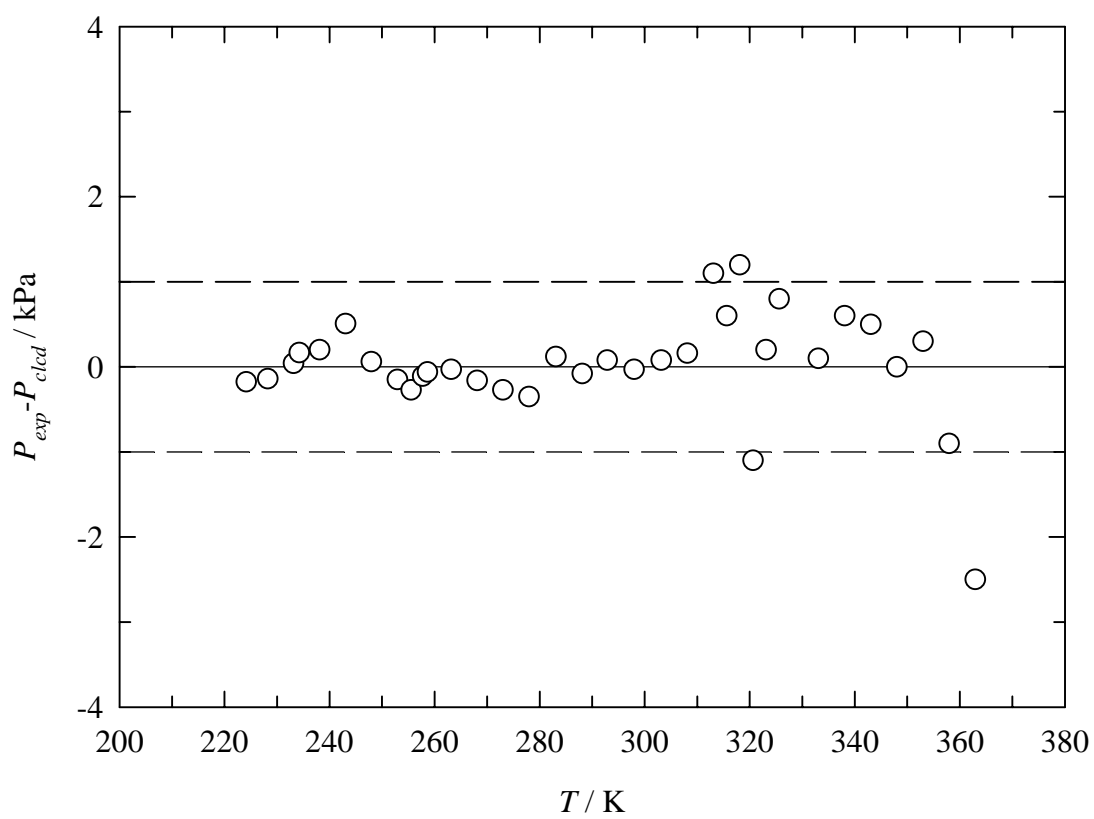


Figure 4.

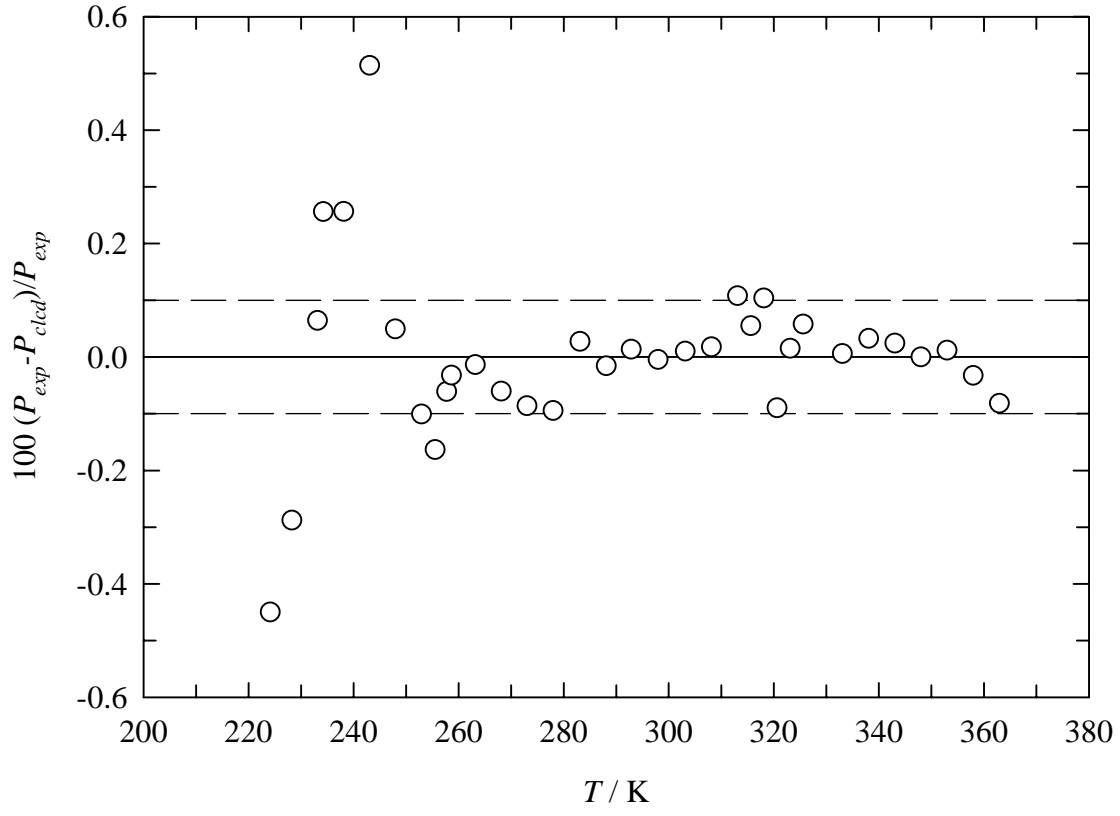


Figure 5.

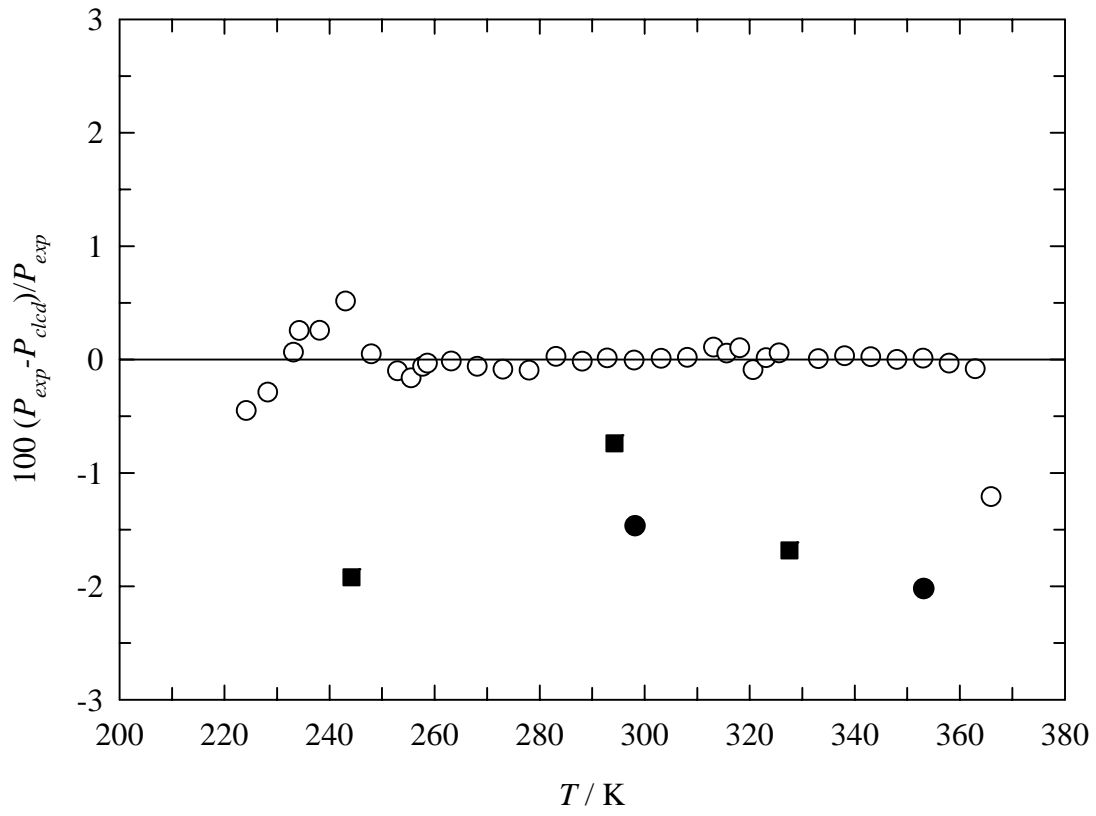


Figure 6.